IL NUOVO CIMENTO **47 C** (2024) 187
DOI 10.1393/ncc/i2024-24187-7

Colloquia: HADRON2023

T_{cc} states of D^*D^* and $D_s^*D^*$ molecular nature

L. R. Dai([1])([*]), E. Oset([2]) and R. Molina([2])

([1]) *School of Science, Huzhou University - Huzhou, 313000, Zhejiang, China*
([2]) *Departamento de Física Teórica and IFIC, Centro Mixto Universidad de Valencia-CSIC Institutos de Investigación de Paterna - Aptdo.22085, 46071 Valencia, Spain*

received 21 December 2023

Summary. — The newly observed T_{cc} state can be explained as a molecular state of D^*D in the chiral unitary approach. An extension to D^*D^* and $D_s^*D^*$ systems in the $J^P = 1^+$ will be discussed in the present work. We make predictions that the D^*D^* system leads to a bound state with a binding of the order of MeV and similar width, while the $D_s^*D^*$ system develops a strong cusp around threshold.

1. – Motivation

The newly observed T_{cc} state is close to the D^*D threshold and the width is very small [1]. This state can be explained as a molecular state of D^*D in the chiral unitary approach [2], both the width and the $D^0D^0\pi^+$ mass distribution are in remarkable agreement with the experiment [1]. In the theoretical framework of D^*D system [2], the chiral unitary coupled channel approach ($D^{*+}D^0$, $D^{*0}D^+$) is utilized and the interaction was obtained from exchange of vector mesons in a straight extrapolation of the local hidden gauge approach. This approach has been successfully applied to the charm sector [3], in which the only parameter was a cutoff regulator in the Bethe-Salpeter equation.

Encouraged by this D^*D work, we make an extension of the above case to D^*D^* and $D_s^*D^*$ systems [4]. There are three reasons for the extension. First, heavy-quark spin symmetry allows to relate the D and D^* sectors. Second, it was also found that the D^*D^* system in $I = 0, J^P = 1^+$, and the $D_s^*D^*$ system in $I = \frac{1}{2}, J^P = 1^+$, both cases have attractive potentials, strong enough to support bound states [5]. Third, the new T_{cc} experimental information can provide valuable information to fix the regulator of the meson-meson loop function [1].

In the present work, since the vector-vector (VV) states with 1^+ cannot decay to pseudoscalar-pseudoscalar (PP) if we want to conserve spin and parity, thus we consider instead the decay into vector-pseudoscalar (VP) channel which will give a width to the bound states that we find.

([*]) E-mail: dailianrong@zjhu.edu.cn

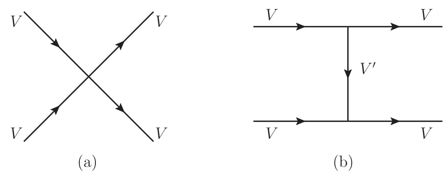

Fig. 1. – Terms for the VV interaction: (a) contact term; (b) vector exchange.

2. – Formalism

The mechanisms for the interaction are depicted in fig. 1, and the corresponding Lagrangians are given:

$$\mathcal{L}^{(c)} = \frac{g^2}{2}\langle V_\mu V_\nu V^\mu V^\nu - V_\nu V_\mu V^\mu V^\nu\rangle, \quad \mathcal{L}_{VVV} = ig\langle V^\mu \partial_\nu V_\mu - \partial_\nu V_\mu V^\mu\rangle, \tag{1}$$

with $g = \frac{M_V}{2f}$ ($M_V = 800\,\text{MeV}, f = 93\,\text{MeV}$), where $\mathcal{L}^{(c)}$ is a contact term and $\mathcal{L}_{VVV}$ stands for the three-vector vertex. The V_μ is the $q\bar{q}$-matrix written in terms of vector mesons

$$V_\mu = \begin{pmatrix} \frac{\omega}{\sqrt{2}} + \frac{\rho^0}{\sqrt{2}} & \rho^+ & K^{*+} & \bar{D}^{*0} \\ \rho^- & \frac{\omega}{\sqrt{2}} - \frac{\rho^0}{\sqrt{2}} & K^{*0} & D^{*-} \\ K^{*-} & \bar{K}^{*0} & \phi & D_s^{*-} \\ D^{*0} & D^{*+} & D_s^{*+} & J/\psi \end{pmatrix}_\mu . \tag{2}$$

The interaction between vectors exchanging vector mesons will generate the bound states or resonances [6, 7]. Extrapolated to the charm sector, it predicted the pentaquark states [3], which were later confirmed by the LHCb experiments [8, 9].

From refs. [6, 7], we can obtain the potential for D^*D^* system,

$$V_{D^*D^*\to D^*D^*} = \frac{g^2}{4}\left(\frac{2}{m^2_{J/\psi}} + \frac{1}{m^2_\omega} - \frac{3}{m^2_\rho}\right) \times \{(p_1+p_4).(p_2+p_3) + (p_1+p_3).(p_2+p_4)\}, \tag{3}$$

and potential for $D_s^*D^*$ system,

$$V_{D_s^*D^*\to D_s^*D^*} = -\frac{g^2(p_1+p_4).(p_2+p_3)}{m^2_{K^*}} + \frac{g^2(p_1+p_3).(p_2+p_4)}{m_{J/\psi^2}}. \tag{4}$$

We further solve the Bethe-Salpeter equation,

$$T = [1 - VG]^{-1}V, \tag{5}$$

with G the loop function which can be regularized by the value of the cutoff.

In order to obtain the imaginary part for the $D^*D^* \to D^*D$ ($I = 0$) case, we consider total 32 decay box diagrams. In fig. 2, where the meaning of the right-hand side is that

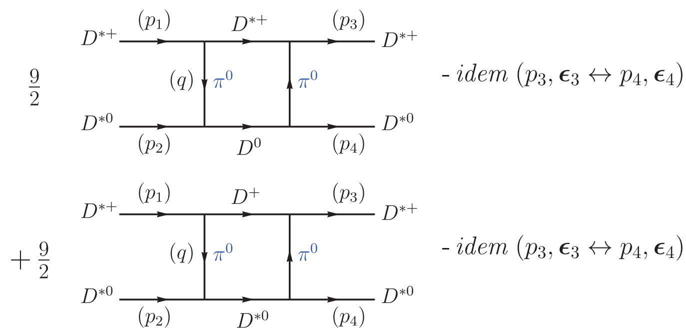

Fig. 2. – Diagrams to be calculated with their respective weights.

the set of diagrams must be completed exchanging the vectors $D^*(p_3) \leftrightarrow D^*(p_4)$ in the final state, given the identity of the two D^* in the final state and when $p_3, \boldsymbol{\epsilon}_3 \leftrightarrow p_4, \boldsymbol{\epsilon}_4$ ($\boldsymbol{\epsilon}_i$ is the polarization vector of particle i) are exchanged, there is a relative (-1) sign [4].

The isospin doublets $(D^+, -D^0)$ and $(D^{*+}, -D^{*0})$

$$|D^*D^*, I=0\rangle = -\frac{1}{\sqrt{2}}|D^{*+}D^{*0} - D^{*0}D^{*+}\rangle. \tag{6}$$

This D^*D^* system can decay into $D^{*+}D^0$ or $D^{*0}D^+$. We find some diagrams with the same structure and only the isospin coefficients are different, thus these diagrams can be classified into 4 kinds with weight of each kind of diagrams $\frac{1}{4}(1+2+2+4+4+2+2+1) = \frac{18}{4} = \frac{9}{2}$.

We find that two new vertices for the box diagrams will need to be evaluated. Finally, using the projectors into the different spin states of $J = 1, 2, 3$, $\mathcal{P}^{(0)}$, $\mathcal{P}^{(1)}$, $\mathcal{P}^{(2)}$, the product of all four vertices will be calculated [6]. Altogether for the $J^P = 1^+$ state, we obtain the contribution for the four diagrams, keeping the positive energy part of the propagators of the heavy particles and performing the q^0 analytically

$$\mathrm{Im}V_{\mathrm{box}} = -\frac{6}{8\pi}\frac{q^5}{\sqrt{s}}E_{D^*}^2(\sqrt{2}g)^2\left(\frac{G'}{2}\right)^2\left[\frac{1}{(p_2^0 - E_D(\boldsymbol{q}))^2 - \boldsymbol{q}^2 - m_\pi^2}\right]^2 F^4(q)F_{HQ}, \tag{7}$$

where

$$q = \frac{\lambda^{1/2}(s, m_{D^*}^2, m_D^2)}{2\sqrt{s}}, \quad F(q) = e^{((q^0)^2 - \boldsymbol{q}^2)/\Lambda^2}, \quad q^0 = p_1^0 - E_{D^*}(\boldsymbol{q}), \quad E_{D^*} = \frac{\sqrt{s}}{2},$$

$$F_{HQ} = \frac{m_{D^*}^2}{m_{K^*}^2}, \qquad G' = \frac{3\,g'}{4\pi^2 f}, \qquad g' = -\frac{G_V m_\rho}{\sqrt{2}f^2}, \qquad G_V = 55\,\mathrm{MeV}.$$

Next we continue to consider another decay box diagrams in fig. 3 to obtain the imaginary part for $D_s^*D^* \to D_s^*D + D_sD^*$ case:

$$\begin{aligned} \mathrm{Im}V_{\mathrm{box}} = &-\frac{1}{3}\frac{1}{8\pi}\frac{1}{\sqrt{s}}(2g)^2\left(\frac{G'}{\sqrt{2}}\right)^2(E_1E_3 + E_2E_4) \\ &\times q^5\left[\frac{1}{(p_2^0 - E_{D_s}(\boldsymbol{q}))^2 - \boldsymbol{q}^2 - m_K^2}\right]^2 F^4(q)F_{HQ}, \end{aligned} \tag{8}$$

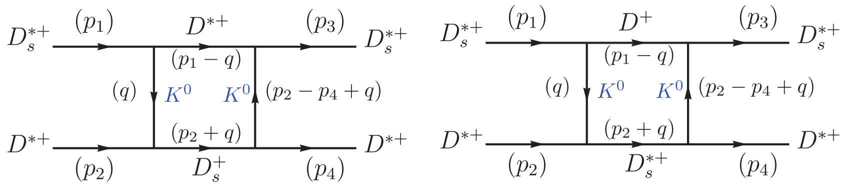

Fig. 3. – Diagrams for the decay of $D_s^{*+}D^{*+}$ into $D_s^{*+}D^+$ and $D_s^+D^{*+}$.

where

$$q^0 = p_2^0 - E_{D_s}(\boldsymbol{q}), \qquad q = \frac{\lambda^{1/2}(s, m_{D^*}^2, m_{D_s}^2)}{2\sqrt{s}}, \qquad p_2^0 = \frac{s + m_{D^*}^2 - m_{D_s^*}^2}{2\sqrt{s}}.$$

3. – Results

Now we will solve the Bethe-Salpeter equation

$$V \to V + i\,\mathrm{Im}V_{\mathrm{box}} \tag{9}$$

to obtain the T-matrix. Further by plotting the amplitudes of $|T|^2$, we obtain the mass of the state and its width.

In fig. 4 we show the predictions for the D^*D^* system, it is seen the bound states with binding of the order of MeV, and the width of the D^*D^* system is much larger than the one of the T_{cc} state, since we have the decay channel D^*D, where there is a much larger decay phase space [4]. As noticed, the width of the T_{cc} state is only 40–50 keV, due to the very little phase space for the $D^* \to D\pi$ decay [2].

In fig. 5 we show the predictions for the $D_s^*D^*$ system, in which no bound state is seen, instead, we find pronounced cusps at the $D_s^*D^*$ threshold. This is a consequence of the weaker potential compared to D^*D^*, because of the different factors of ImV_{box} from π exchange and kaon exchange, respectively.

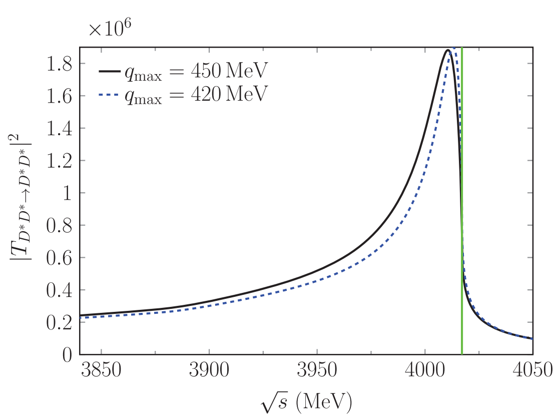

Fig. 4. – The amplitudes $|T|^2$ at $q_{\max} = 420$ MeV and $q_{\max} = 450$ MeV, the vertical line shows the threshold of D^*D at 4017.1 MeV.

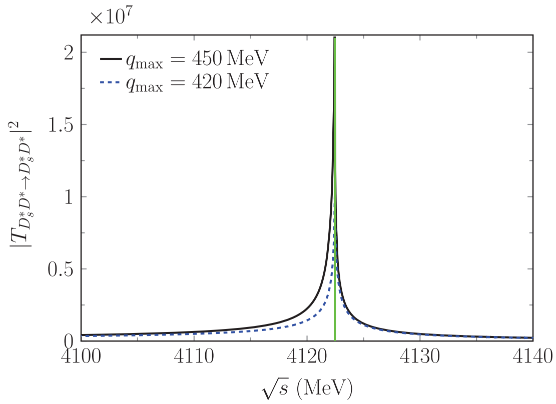

Fig. 5. – The amplitudes $|T|^2$ at $q_{\max} = 420$ MeV and $q_{\max} = 450$ MeV, the vertical line shows the threshold of $D_s^*D^*$ at 4122.46 MeV.

4. – Summary

Encouraged by the experiment of the T_{cc} state close to the D^*D threshold, which can be explained as a molecular state of D^*D in the chiral unitary approach, we made an extension to D^*D^* with $I = 0$ and $D_s^*D^*$ with $I = \frac{1}{2}$ systems to investigate the possible existence of bound states or resonances. We use the new experimental information from the T_{cc} state to fix the cutoff and then evaluate the decay box diagrams to get the width. We find the bound state of the D^*D^* system with a binding of the order of MeV and its width is much larger than the one of the T_{cc} state. The $D_s^*D^*$ system develops a strong cusp around threshold, and its width is much smaller than that of the D^*D^* state due to the different exchanges from pion and kaon, respectively.

* * *

The authors acknowledge supports partly from the National Natural Science Foundation of China under Grants Nos. 12175066 and 11975009.

REFERENCES

[1] LHCb Collaboration (Aaij R. *et al.*), *Phys. Rev. Lett.*, **125** (2020) 242001.
[2] Feijoo A., Liang W. H. and Oset E., *Phys. Rev. D*, **104** (2021) 114015.
[3] Wu J. J., Molina R., Oset E. and Zou B. S., *Phys. Rev. Lett.*, **105** (2020) 232001.
[4] Dai L. R., Molina R. and Oset E., *Phys. Rev. D*, **105** (2022) 016029; **106** (2022) 099902(E).
[5] Molina R., Branz T. and Oset E., *Phys. Rev. D*, **82** (2010) 014010
[6] Molina R., Nicmorus D. and Oset E., *Phys. Rev. D*, **78** (2008) 114018.
[7] Geng L. S. and Oset E., *Phys. Rev. D*, **79** (2009) 074009.
[8] LHCb Collaboration (Aaij R. *et al.*), *Phys. Rev. Lett.*, **115** (2015) 072001.
[9] LHCb Collaboration (Aaij R. *et al.*), *Phys. Rev. Lett.*, **122** (2019) 222001.